Turkish Journal of Civil Engineering, 2023 59-78, Paper 717, ***Research Article***

An Experimental and Numerical Investigation on the Bending Behavior of Fiber Reinforced Concrete Beams

Mehmet Alper ÇANKAYA[1]
Çetin AKAN[2]

ABSTRACT

The effects of hooked end steel and polypropylene (PP) fibers on the behavior of large-scale doubly reinforced concrete beams under flexure were investigated using experimental and numeric methods. For this purpose, a total of eight beam specimens consisting in two groups were produced in the laboratory and three-point bending tests were conducted under monotonically increasing load. The beams in the groups were designed to have 0.86 and 1.30% tensile reinforcement ratios leading to either flexural or shear critical sections. Three out of eight were produced to be control samples and did not have any fiber additive while remaining five had 0, 0.5 and 1.0% steel or PP fibers by volume. Experimental results showed that the existence of 0.5% either type of fiber in densely reinforced specimens contributed to shear strength and allowed flexural capacities to be fully used instead of an improvement in the capacity. However, when the steel fiber ratio increased to 1.0% flexural capacity was enhanced by 10% for both type of beams. After the experimental study, the beams numerically modeled using nonlinear finite element method and flexural stiffness before yielding as well as yield strength with load carrying capacities were found to be consistent with that of experiments specifically for the beams having stirrup and steel fibers.

Keywords: Fiber reinforced concrete (FRC), bending behavior of FRC beams, polypropylene and hooked end steel fibers, nonlinear finite element analysis.

1. INTRODUCTION

Fiber reinforced concrete (FRC) has been widely used in non-critical members of civil engineering structures basically for crack control and durability [1]. Precast tunnel lining segments, concrete pavements and industrial building floors are some of the application areas

Note:
- This paper was received on October 25, 2021 and accepted for publication by the Editorial Board on October 10, 2022.
- Discussions on this paper will be accepted by March 31, 2023.
- https://doi.org/10.18400/tjce.1209152

1 Izmir Katip Celebi University, Department of Civil Engineering, İzmir, Türkiye
mehmetalper.cankaya@ikcu.edu.tr - https://orcid.org/0000-0002-5491-3425

2 Izmir Katip Celebi University, Department of Civil Engineering, İzmir, Türkiye
Y190227018@ogr.ikcu.edu.tr - https://orcid.org/0000-0003-2807-4266

of FRC. Although FRC was being used only for crack width control initially, it has been started to be considered in the strength analysis of structural members [2]. However, the full potential of FRC is not still being used such as fully or partially replacement of costly and labor-intensive shear reinforcements [3].

In the literature, many studies have been undertaken regarding the shear and flexural characteristics of FRC members more specifically on the steel fiber reinforced concrete beams [3-9]. Studies concerning the shear strength revealed that elimination of stirrups is possible when hooked-type steel fibers in a volume ratio of at least 0.75% are included in the normal and high strength concrete [10, 11]. However, increasing the volumetric ratio of fibers up to 2.0% or higher might end up with a less ductile failure type [12] depending on the shear length to effective depth ratio [7]. Apart from the contribution to shear, inclusion of steel fiber was also found to be beneficial in terms of cracking and deformational behavior of RC beams subjected to flexure [8, 9]. The existence of steel fibers inhibited crack propagation, decreased the width, length and spacing of cracks [9, 13]. Additionally, it enhanced the flexural rigidity at any given load level [8] and therefore, deflection and strain in reinforcing steel substantially reduced. Besides, steel fibers were found to be effective in increasing the yield and ultimate bending moment capacity of the RC beams [7, 14]. Moreover, SFRC shows significant ductility at failure [15]. The efficiency of steel fibers regarding the performance and behavior of RC members also depends on the longitudinal reinforcement ratio. Specifically, in lightly reinforced RC beams the effect was detected to be more pronounced [13, 16] compared to that of heavily reinforced sections. However, in either case this observation was made for the beams designed to be critical in flexure and premature shear failure was prevented by providing shear reinforcements into the shear span.

PP fiber is a synthetic type of fiber with low density and modulus of elasticity [17]. From the conducted studies it was detected to be beneficial to increase the tensile and flexural strength, providing resistance to shrinkage cracking as well as good toughness in concrete structures [18-22]. In the literature it is also possible to encounter with a comparison of effect of different types of fibers into the mechanical behavior RC beams. For example, the structural tests were conducted in the study performed by [23] using hooked-end steel, PP and hybrid types of fibers. Based on the results of beam specimens failed from flexure, it was observed that the beams having 1.1% PPF exhibited a higher ductility compared to that of beam having 2.0% steel fibers for a specific amount of longitudinal reinforcement ratio. However, an opposite conclusion was reported in another experimental study [24] which can be interpreted as there is no consensus on the issue.

A significant amount of work has been conducted to investigate the effects of fibers on the behavior of RC members but very few studies [6, 10 and 11] were performed on the full or large scale, doubly reinforced RC beams similar to that of practical applications. Moreover, longitudinal reinforcement ratio as a variable was generally investigated on the beams designed to perform full flexural capacity. The current study aims not only providing an experimental insight into the effects of fiber ratio and type on the shear and flexural critical beam behavior but also attempts to understand the appropriateness and limits of selected numerical approach in modeling. For this purpose, a total of eight doubly reinforced, large-scale concrete beam specimens were constructed at the Structural Mechanics Laboratory of İzmir Katip Çelebi University and three-point bending tests were carried out under monotonically increasing load. Fiber volume fractions (V_f) and type were selected to be the

main variables. Additionally, the beam specimens were designed to have two different tensile reinforcement ratios leading to either shear or flexure critical sections. Three out of eight were selected to be control specimens while the remaining five had varying volumetric fiber ratios. Except one of the beams in the control specimens, none of them had stirrups to observe the behavior free from the shear reinforcement effect. Once the experimental study completed, modified compression field theory (MCFT) based non-linear finite element (NLFE) analysis was conducted using VecTor2 [25] software. Force versus mid-span deflection curves and crack profiles were compared with that of the experiment.

2. EXPERIMENTAL STUDY

To investigate the behavior of FRC beams, eight large-scale and doubly reinforced beam specimens having 20 mm typical clear concrete cover were produced and tested, as shown in Figure 1. All the specimens had 150x200x2450 mm prismatic geometry and consisted of two groups. The first group (B1 series) was designed to have 1.30% tensile reinforcement ratio while the second group (B2 series) had 0.86% as can be seen in Figure 1. Two of those reinforcements were equipped with strain gauges from the mid-length of each beam specimen. Thus, the force occurring on the rebars could be followed. Two beams from B1 series were selected to be control specimens. One of which had a minimum shear reinforcement ratio according to TS500 [26] and calculated from Equation (1). However, rest of the specimens, including the remaining control beam, did not have any stirrups. In Equation (1), A_{sw}, b_w, s, f_{ctd} and f_{ywd} are shear reinforcement area, web thickness, spacing between stirrups, design tensile strength of concrete and design yield strength of shear reinforcement, respectively. Calculated minimum shear reinforcement ratio (0.95×10^{-3}) consequently led "s" to exceed the maximum spacing dictated by TS500 as half effective depth (d/2). Therefore, the distance between each stirrup was taken as d/2.

$$\rho_{min} = \frac{A_{sw}}{b_w s} = 0.30 \frac{f_{ctd}}{f_{ywd}} \quad (1)$$

Table 1 - Specimen reinforcement and fiber ratios

Beam Specimen	Longitudinal Reinforcement (Bottom and Top)	Tensile Reinforcement Ratio	Fiber Type and Volumetric Ratio (%)
B1- Control w/o str	3Ø12 - 2Ø12	0.0130	No fiber
B1-Control w/str	3Ø12 - 2Ø12	0.0130	No fiber
B1-SF05	3Ø12 - 2Ø12	0.0130	Steel - 0.5
B1-SF10	3Ø12 - 2Ø12	0.0130	Steel - 1.0
B1-PPF05	3Ø12 - 2Ø12	0.0130	PP – 0.5
B2-Control w/o str	2Ø12 - 2Ø12	0.0086	No fiber
B2-SF10	2Ø12 - 2Ø12	0.0086	Steel – 1.0
B2-PPF05	2Ø12 - 2Ø12	0.0086	PP – 0.5

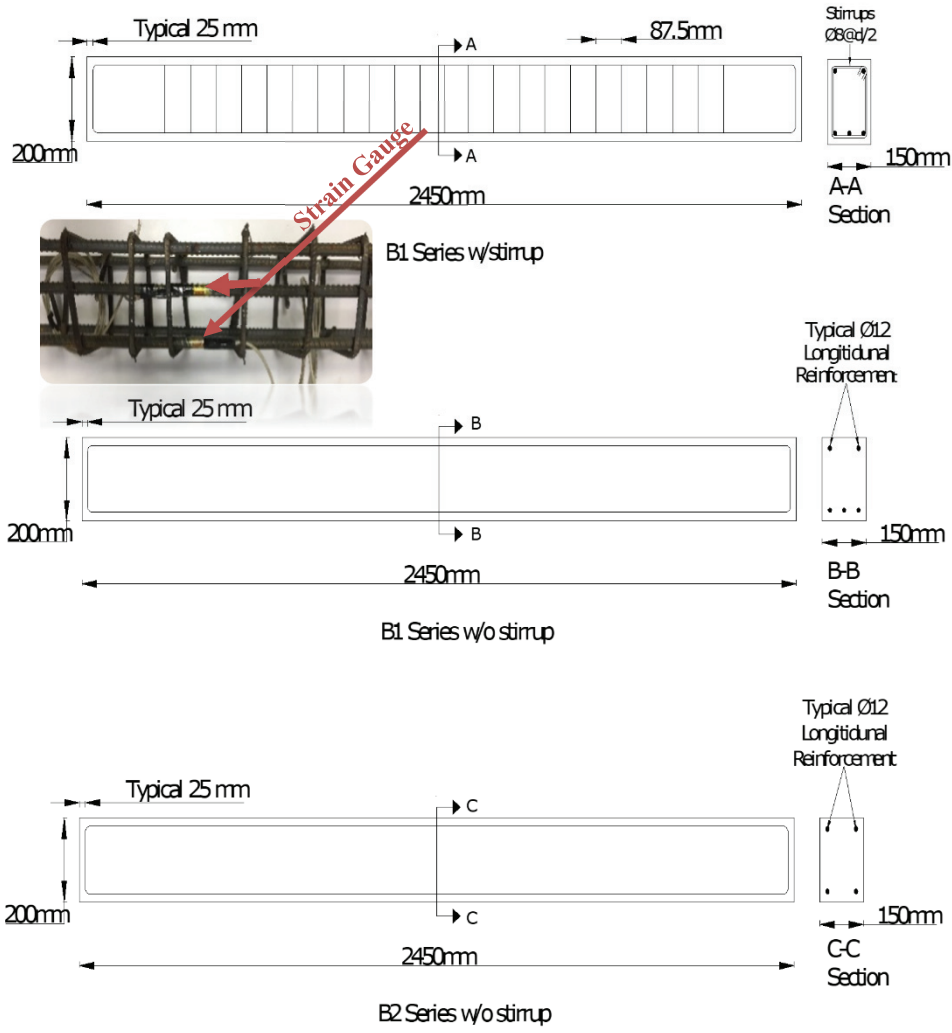

Figure 1 - Side-view and cross sections of specimen groups

Relatively low tensile reinforcement ratio in B2 series caused a tendency to flexural type of failure. Therefore, the effectiveness of stirrups was not investigated in B2 series. As a result, only one beam was selected to be the control specimen without stirrup. None of the control beams had fiber content while the remaining beams had various ratios of steel and PP fibers. A detailed list of beams that includes the fiber reinforcement type and ratio is presented in Table 1.

According to naming convention given in Table 1, first letter and the following number stand for the group of beams related to tensile reinforcement ratio. The letters with numbers after

the group name represent the type and ratio of fiber reinforcement. For example, B1-SF05 is for the beam having 1.3% tensile reinforcement and V_f=0.5% steel fiber. In the current study, the ratio of shear span (a=1000 mm) to effective depth (d= 174 mm) was calculated to be 5.75 for both B1 and B2 series. This ratio yields to either diagonal tension failure or flexural failure in the beams that does not have any stirrups or fibers depending on the flexural capacity provided by tensile reinforcement.

Commercially available B420C grade deformed bars were ordered and used for longitudinal and shear reinforcements. Yield and ultimate strength of reinforcements were obtained through the tension tests as 500 and 670 MPa, respectively. Three 30-cm long coupons were used for the tests and the average of the results was taken. On the other hand, necessary limited volume of each batch of concrete was mixed in the laboratory utilizing a concrete mixer and poured into the formworks, as shown in Figure 2. ACI 211.1 [27] code, which is nearly identical to TS-802 [28], was followed to determine mixture ingredients and proportions of concrete considering slump, maximum aggregate size, mixing water, air volume, water/cement (W/C) ratio, cement and aggregate amount. According to sieve analysis maximum aggregate size was detected as 16 mm and W/C ratio was selected based on the aimed strength (at least 20 MPa cylinder compressive strength) of concrete. Mixture design is given in Table 2.

Figure 2 - Steps of concrete pouring

Table 2 - Mix proportions of concrete

W/C ratio	Cement content (kg/m^3)	Water (kg/m^3)	Aggregate (kg/m^3)	Steel Fiber (kg/m^3)	PP Fiber (kg/m^3)	Air content
0.55	414.5	228.0	1557	39.25 and 78.50 (0.5% and 1.0%)	4.550 (0.5%)	2.5%

The workability of concrete decreased during the pouring process as the fiber content increased. Such an observation was also reported by [22]. Therefore, a proper vibration was given to the fresh concrete in the formworks. Next, concrete samples were randomly taken from different batches to perform compression tests. Six standard cubes were used for this purpose. The cube samples were kept by the beam specimens in the same curing conditions with beam specimens. Once the concrete hardened the formworks were removed. Afterwards, the cubes and beam specimens were wrapped with cloth sheeting and then the surfaces were properly ponded with water for 28 days. Compression tests of cube samples were performed at the day of experiment which is not less than 28 days after casting. Strength values of the cube samples were converted to equivalent cylinder values by multiplication of 0.85 based on [29]. Mean cylinder strength of the concrete was calculated as 25 MPa. Hooked end type "Betonfiber 1050" steel, and "Betonfiber BF19" polypropylene (PP) fibers were used in the study and the mechanical and geometric properties were obtained from the manufacturer and presented in Table 3.

Table 3 - Physical properties of fibers

Material	Length (mm)	Diameter	Density	Tensile Strength
Steel Fiber	50 mm	1.0 mm	7850 kg/m^3	1100 MPa
PP Fiber	19 mm	20 μm	910 kg/m^3	575 MPa

Figure 3 - Overview of test setup (left) and instrumentation for experiments (right)

Static three-point bending test setup is given in Figure 3. As seen from the figure above, beam specimens were placed into the rigid frame and clear span between roller and pin supports was 2000 mm. The beams were pushed downwards by a single load from the mid-span using a 300 kN capacity hydraulic jack. A load cell was placed under the hydraulic jack for

detecting the load exerted to beam, and mid-span deflection was monitored via two linear resistance potentiometer transducers (LRPT). The sensors were connected to an 8-channel data acquisition device for gathering the data.

The loading protocol was monotonic until the empirically calculated plastic moment capacity (M_p) is reached in the experiments except for B1 and B2 cases without stirrup. The specified load is regarded as load carrying capacity of each test specimen. M_p was calculated based on Equation (2) as given in Turkish Seismic Code 2018 [31].

$$M_p = 1.4M_r \tag{2}$$

Due to the complexity in calculating the ultimate moment capacity (M_r) of the beams having fiber additive, an approximation was made in Equation (2) by replacing M_r with yield moment capacity (M_{ry}). However, it is understood from the study performed by [32] such a simplification will end up with a higher capacity than it is supposed to be, specifically for the beams having relatively high tensile reinforcement ratio. As reported in [32] the error could be up to 15%. Considering this error, the capacity was defined to be $1.20M_{ry}$ in the current study. Consequently, the experiments were stopped when the load exceeded the yield capacity by 20%.

3. RESULTS AND DISCUSSION

3.1. Sectional Analysis

Beam sections of the control specimens without stirrup were analyzed to capture yield and ultimate moment capacities. Contribution of tension stiffening effect and strain hardening in rebars were considered in the analyses. As it can be seen from Figure 5, in the experiments tension reinforcements yielded at an approximate strain of 2.5×10^{-3}. This value corresponds to 500 MPa tensile stress and used in the cross-sectional analysis. Concrete crushing strain was taken to be 3.0×10^{-3} as suggested in TS500. In both beam types, tension reinforcements were detected to be yielded before the compression crush of concrete. In addition to flexural analysis, diagonal tensile (shear) strength of beams was also calculated. For this purpose, Equation (3) suggested by ACI 318-19 [30] code was used since size effect (depth of member) and contribution of longitudinal reinforcement ratio on shear strength are taken into consideration.

$$V_c = 0.66\lambda_s\lambda\rho^{1/3}\sqrt{f_c'}b_w d \tag{3}$$

In the equation, V_c, λ_s, λ, ρ, f_c', b_w and d represent shear strength of concrete, size effect factor, modification factor for concrete material, tensile reinforcement ratio, compressive strength of concrete, width of beam and effective depth, respectively. Based on the findings in sectional analyses, shear failure type is expected for B1 control specimen since the load carrying capacity provided by shear strength of the beams is less than that of flexure. However, the capacities gathered from flexure and shear were approximate to each other for B2 control specimen, therefore, a specific failure type could not be estimated. Analysis results are tabularized in Table 4 and further details of flexural analysis can be found in [33].

Table 4 - Sectional analysis of control specimens

Specimen	Flexure				Shear		Expected type of failure
	M_{ry} (kNm)	P_{ry} (kN)	M_r (kNm)	P_r (kN)	V_s (kN)	P_s (kN)	
B1 Control w/o Stirrup	25.6	51.3	27.1	54.2	20.2	40.5	Shear before yield
B2 Control w/o Stirrup	18.4	36.9	19.8	39.5	17.7	35.4	Flexure and/or shear

*P_{ry} and P_r are yield and ultimate load capacities, respectively. V_s and P_s are shear strength and corresponding point load.

3.2. Behavior under Load

The load-midspan deflection curves of the tested beams were presented in Figure 4 to investigate the behavior under loading. It can be deduced from the curves that B1 control specimen w/o stirrup yielded at 44.0 kN. However, the yield strength was detected to be 51.3 kN in the pure flexural analysis of cross-section, indicating an error of 16%. The reason for this error can be attributed to additional strain on longitudinal reinforcements caused by shear [34]. Due to safety concerns and expectation of brittle type of failure, the experiment was stopped when the load reached to 48.5 kN and a corresponding mid-span deflection of 20 mm. Therefore, 48.5 kN is assumed to be the experimental load carrying capacity of the specimen in the study. On the other hand, introducing a minimum amount of shear reinforcement (B1 control w/stirrup), 0.5% steel (B1-SF05) and PP (B1-PPF05) fibers did not promote the yield moment capacity, but instead, allowed the beams to fully employ their yield moment capacity by reaching a load almost identical to that of flexural analysis as 51.0 kN. In other words, the shear critical behavior of those beams shifted into the flexural. However, increasing the volumetric ratio of steel fibers to 1.0% did not only transform the shear critical behavior into flexural but also slightly enhanced the yield loading (10%) of B1-SF10 specimen, basically depending on the increase in the moment capacity of the cross-section. Such an enhancement in moment capacity was also reported by [23] on the moment-curvature diagrams of beams including 2.0% and 1.1% steel and PP fibers. Loading of beams continued after yielding and resulted in strain hardening of reinforcements. Strain hardening behavior consequently increased the load carrying capacity of members rapidly until crushing of the outermost shell of concrete and resulted in a minor reduction in load carrying capacity, see Figure 4 (left). Of course, this is not the case for B1 control w/o stirrup since the loading was stopped at relatively earlier stage. As previously mentioned, the tests were continued until 1.20 times of yield strength, which was regarded as load carrying capacity. Three beam specimens, namely: B1 control w/stirrup, B1-SF05, and B1-PPF05, attained load-carrying capacities in the vicinity of 60.0 kN. This is equal to the analytically calculated capacity ($1.20P_{ry}$) of B1 control w/o stirrup but at least 1.25 times that of the experiment. As expected, B1-SF10 beam specimen performed the highest bearing capacity compared to the remaining beams of the B1 series and enhanced the load carrying capacity by 10% with respect to the specimens that can fully use their flexural capacity.

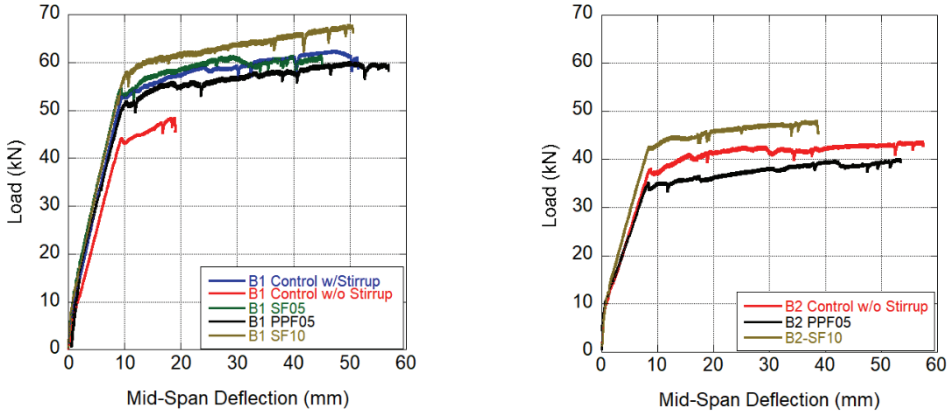

Figure 4 - Load-displacement curves of B1 (left) and B2 (right) series

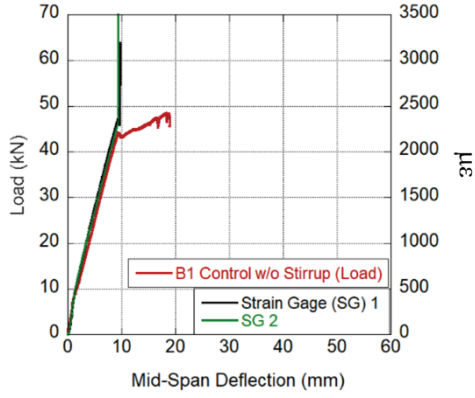

Figure 5 - Relationship of midspan deflection with load and rebar strain history

In B2 series, lower tensile reinforcement ratio resulted in a dominating flexural behavior and led control specimen to employ fully its yield strength by reaching 37.0 kN being identical to that of analytically calculated case. The experiment of this specimen was stopped at 42.0 kN load corresponding to $1.13M_{ry}$ instead of $1.20M_{ry}$. This was mainly to prevent a sudden failure since the strength provided by flexural and shear capacities was in proximity with each other though the specimen was fully used its yield moment capacity. Existence of 1.0% steel fibers in B2-SF10 beam has increased the yield load capacity approximately by 8% compared to the experimentally and analytically detected yield loading capacity of B2 control w/o stirrup. Interestingly, a slight reduction approximately 7% in the yield load capacity of B2-PPF05 beam was noticed. The reason for this might be explained by reduced compressive strength of fiber reinforced concrete mixture as detected in [35] depending on a higher porosity and air content in the matrix as reported in [36]. Load carrying capacity was observed to be highest for the specimen having 1.0% steel fiber. It is 1.10 times that of B2

control specimen experimental and analytical results. In fact, the enhancement in load capacity was found to be identical with that of B1-SF10 beam. Such an increase in the ultimate strength was also reported in the parametric study conducted by [14] for the large-scale and normal-strength concrete beams which were designed to fail in flexure. The enhancement was detected to be 11, 12, and 8.0% for the beams having 1.00% steel fiber and 1.18, 1.77, and 2.37% longitudinal reinforcement ratios, respectively. Therefore, it is understood that the strength improvement is almost free from the reinforcement ratio based on the findings of [14] and the current study. The minor reduction in the capacity of specimen having 0.5% PP fiber did not change throughout the loading history and kept 7% decrease in load bearing capacity compared to B2 control beam.

3.3. Ductility

Ductility index (μ) of a beam was defined as the ratio of the deflection at load carrying capacity to the deflection in which the specimens ceased to exhibit their linear behavior. Table 5 summarizes the ductility index values of whole specimens.

Table 5 - Ductility index of B1 and B2 series

Specimen	B1 Control w/o str.	B1 Control w/str.	B1 SF05	B1 SF10	B1 PPF05	B2 Control w/o str.	B2 SF10	B2 PPF05
Ductility index (μ)	2.00	4.77	4.45	5.00	5.68	7.12	4.75	6.80

In B1 series, all the specimens having fiber content performed better ductility response when compared to B1 control w/o stirrup. Interestingly, the highest ductility performance was observed at B1-PPF05 specimen. In other words, PP fibers provided better ductility response compared to that of the beam having a minimum shear reinforcement ratio based on TS500 and steel fiber. A similar finding was indicated in [35] for the full-scale beams that were critical in flexure. In the study, the specimen having 1.0% PP fiber performed superior ductility performance not only against the beams having 0.5 and 1.0% SF but also the beam with stirrup. On the other hand, it can be said that addition of 0.5% steel fibers also improved the ductility quite good and exhibit almost identical performance relative to the beam having minimum amount of shear reinforcement (B1 Control w/stirrup). Increasing the steel fiber ratio to 1.0% caused a very limited contribution (12% enhancement) on the ductility when compared to addition of 0.5% steel fiber. Ductility also affected by the ratio of tensile reinforcement and was greatly enhanced in B2 series except B2-SF10 beam. However, fibers were detected to have reverse effect when compared to B1 series since the ductility of specimens having fibers in B2 series was below the control specimen. Therefore, it can be concluded that depending on the tensile reinforcement ratio fibers decreased the ductility performance of beams. On the other hand, as in B1 series 0.5% PP fiber provided higher ductility than that of specimen having 1.0% steel fiber.

3.4. Crack Patterns

The final state of crack patterns is presented in Figure 6 and 7 for B1 and B2 series respectively. As can be seen from Figure 6, in B1 control beam w/o stirrup a major flexural crack (2-3 mm wide) was observed in the maximum moment region by some additional hairline thick flexural-shear cracks distributed along the length of beam.

Figure 6 - Final state of crack patterns in B1 series

Widespread and almost equally spaced, hairline thick flexural cracks shifting to inclined shear cracks were observed on both sides of the B1 control specimen w/stirrup. Additionally, major flexural cracks (4-5 mm thick) starting from the bottom towards the load were noticed specifically at the loading cone. Shear cracks were more prominent in B1-SF05 specimen compared to B1 control w/stirrup as shown in Figure 6. Formation of approximately 1 mm wide and symmetrically located shear cracks on both sides were detected as well as hairline thick web shear cracks along the beam length. In the loading zone of both sides, flexural cracks reached the width of 5 mm identical to B1 control specimen w/stirrup. When it comes to B1-SF10 specimen, approximately 2 mm thick and symmetrically located flexural-shear cracks were observed on both sides of the specimen in addition to web shear cracks identical to B1-SF05. Again, major flexural cracks such as 3 to 5 mm wide were observed in both faces of the beam specifically at the loading cone. However, in B1-SF10 specimen the

number of crack formation decreased while only a few cracks widen significantly more than the other cracks compared to B1-SF05 and B1 control w/stirrup (Figure 6). This is consistent with the findings of [1]. In B1-PPF05 specimen, the total number of cracks spreading on the sides slightly increased when compared to the beams having steel fiber (Figure 7). In fact, the reason for this might be the higher deformation level as well. However, most of the cracks were in web shear crack form similar to that of beams having steel fiber. Another interesting point was observing narrower flexural cracks (~2mm) especially in the loading cone. As in B1 series beams, most of the major cracks in B2 control specimen w/o stirrup were located in the loading cone. These were 2 to 3 mm wide flexure and flexural-shear cracks in both sides of the beam. Other than that, widely distributed hairline thick flexural-shear cracks were observed. However, in B2-SF10 beam cracks were formed less in quantity specifically on one side compared to control specimen, and they were concentrated in the loading region. Maximum width of flexural cracks detected was 2 to 4 mm. Shear cracks were in the vicinity of 1 mm. In B2-PPF05 the shear cracks observed in the loading region were more prominent, which is reaching to 2~2.5 mm, relative to B2-SF10.

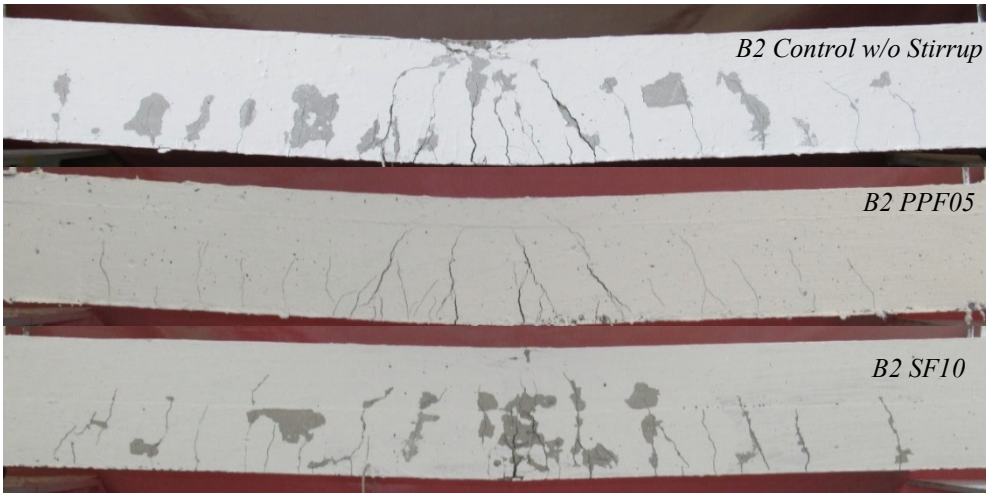

Figure 7 - Final state of crack patterns in B2 series

4. NUMERICAL MODELING AND COMPARATIVE RESULTS

Three-point bending test simulations were conducted by VecTor2 (VT2) [25] software. It is a two-dimensional nonlinear finite element code developed for the analysis of RC members in plane stress conditions and based on Modified Compression Field Theory (MCFT) formulations [37]. This theory is an analytical tool for predicting the load-deformation response of RC membrane elements subjected to shear and normal stresses. It is a combination of three sets of relationships, namely: (1) compatibility conditions of concrete and reinforcement average strains, (2) equilibrium conditions relating the external loads and internal resisting forces in concrete and reinforcement and (3) constitutive relationships which are required to provide a connection between average stresses in the equilibrium relations and average strains in the compatibility relationships for both the reinforcement and

the concrete. Further details of the theory and finite element implementation can be found in elsewhere [25, 37].

Full-scale models of the beam specimens were created using preprocessor FormWorks [25] software. In the analyses, concrete and rebars were modelled using four-node plane stress rectangular elements and two-node truss bar elements, respectively. Between concrete and rebars perfect bond assumption was made and truss elements of rebars shared the same node with that of rectangular elements of concrete. Selected constitutive models for concrete and steel reinforcement is presented in Table 6. The compressive strength of concrete, yield, and ultimate strength of steel rebars as well as length, diameter and tensile strength of fibers were taken from the conducted material tests. Rest of the required parameters were taken as software default which can be found out in [25].

Table 6 - Selected constitutive models for materials used.

Material and property	Model
Concrete - Compression Pre-Peak	Beams w/o fibers: Hognestad (Parabola) Beams w/SF and PPF: Lee et al 2011 (FRC) Beams w/PPF: Popovics (NSC)
Concrete - Compression Post-Peak	Beams w/o fiber: Modified Kent-Park Beams w/SF: Lee et al 2011 (FRC) Beams w/PPF: Montoya 2003
Concrete – Compression Softening	Vecchio 1992-A (e1/e2 form)
Concrete – Tension Stiffening	Beams w/o PP fibers: Lee 2010 (w/Post Yield) Beams w/PP fiber: Modified Bentz 2003
Concrete – Tension Softening	Beams w/o fiber: Linear Beams w/PP fiber: Bilinear Beams w/steel fibers: Exponential
FRC Tension	SDEM – Monotonic
Steel Reinforcement - Dowel Action	Tassios (Crack Slip)
Steel Reinforcement -Buckling	Akkaya 2012 (Modified Dhakal - Maekawa)

* *FRC and NSC stand for fiber reinforced concrete and normal strength concrete.*

Pin and roller supports of the beam specimens were not explicitly modeled, instead; translational restraints were assigned in X, Y and Z directions and the beam specimens were subjected to monotonically increasing deflection (0.1 mm increments) from the mid-span until failure. The optimum mesh density was selected based on the mesh sensitivity analysis as 15 mm with a limitation in the aspect ratio to be two.

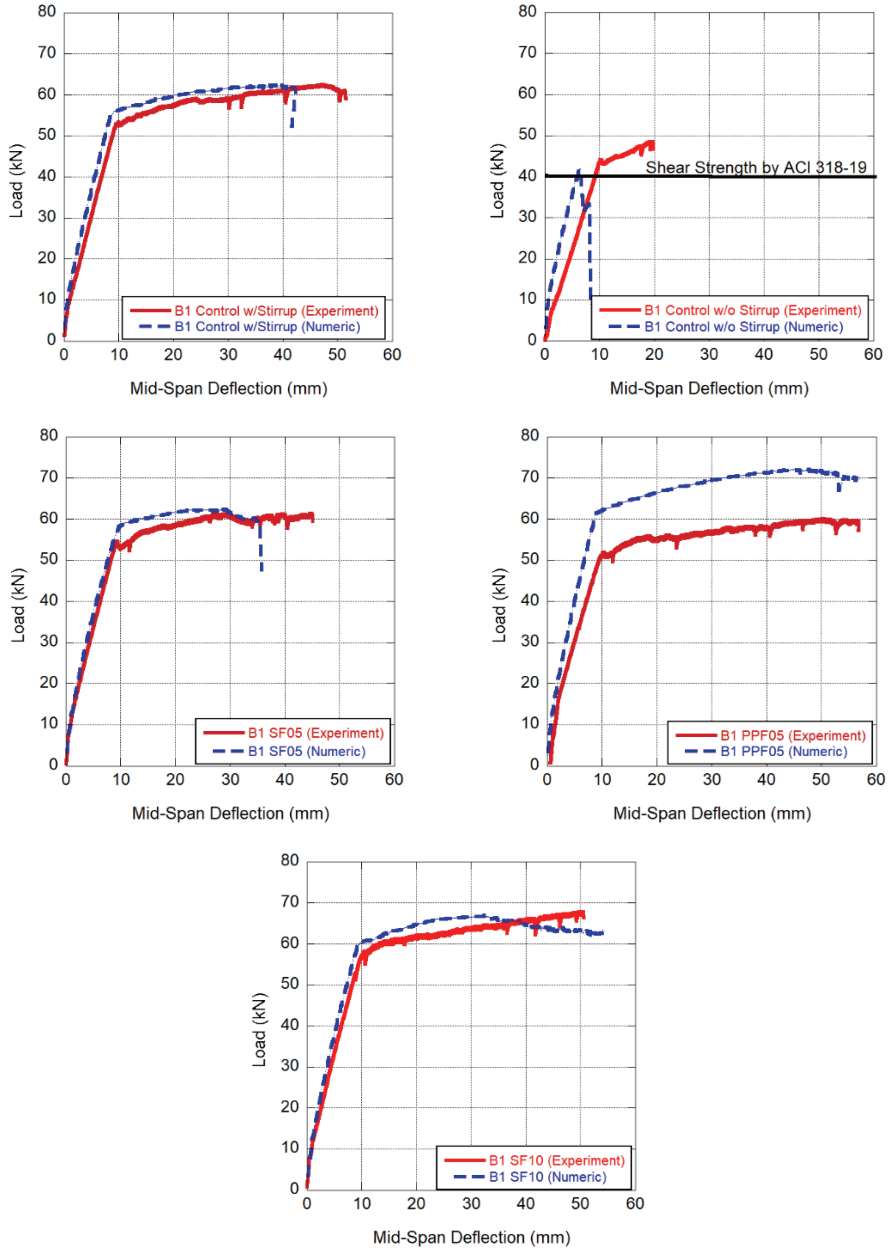

Figure 8 - Comparison of numerical and experimental results for load-deflection curves of B1 series

Numerically and experimentally obtained load-deflection responses of B1 series are presented comparatively in Figure 8 and crack patterns are given in Figure 9. In the analysis, the yield strength and load carrying capacity of B1 control beam w/stirrup was estimated

quite close but with a slight overestimation to that of experiment (Figure 8). Additionally, flexural stiffness before yielding was also in close proximity with that of experiment. This was observed from the slope of load-deflection responses. Similar to the experiment the major flexural and flexural-shear cracks were located in the maximum moment region and consequently flexural failure was observed in the numerical analysis as seen in Figure 9. On the other hand, numerical analysis results of B1 control beam w/o stirrup indicated a premature failure before yielding of tensile reinforcements which is a sign of brittle shear fail. In fact, this coincides well with that of analytically calculated shear strength being less than the flexural capacity. Moreover, the crack pattern obtained through numerical analysis also confirmed a shear failure by diagonal (shear) cracks located on the web, Figure 9. Finally, the flexural stiffness of this beam was calculated to be 1.35 times higher than that of experiment. The reason for higher stiffness can be attributed to the difference between the obtained crack patterns of the experiment and analysis.

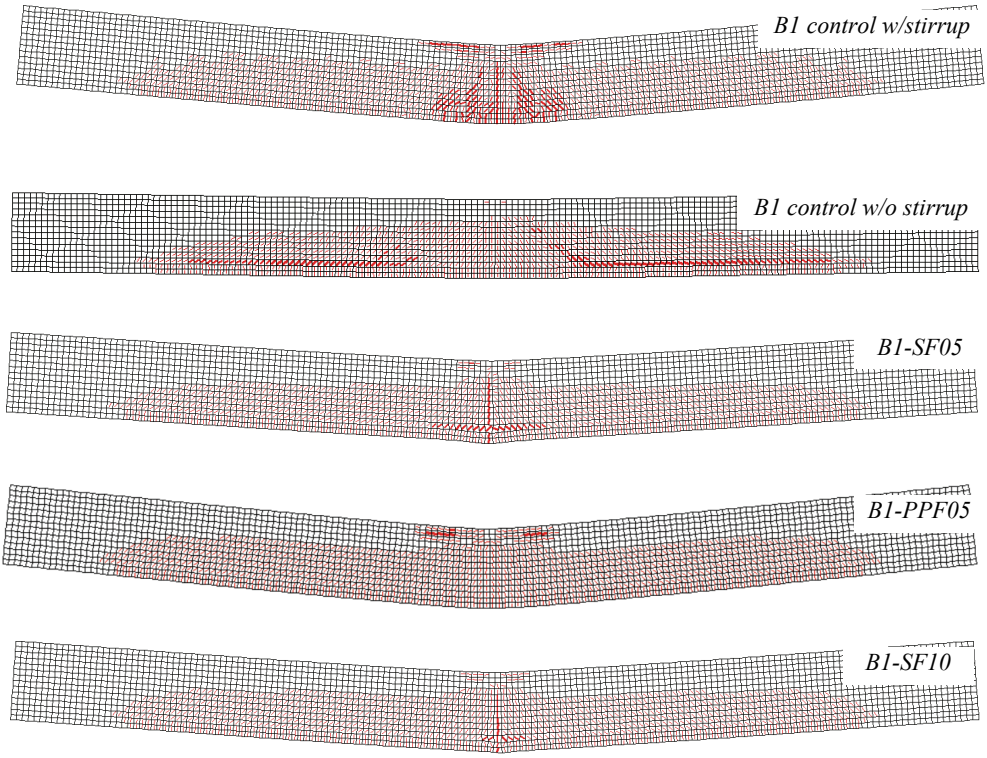

Figure 9 - Crack patterns of B1 series corresponding to peak load

Figure 8 shows that the existence of any type of fiber prevented the premature shear failure and allowed the tensile reinforcements to be yielded. In the analysis of beams having 0.5 and 1.0% steel fiber, the yield strength and corresponding deformation as well as the load carrying capacity and flexural stiffness were satisfactorily captured by a slight and negligible overestimation. However, the yield strength, load carrying capacity and flexural stiffness

were estimated above from the experimental results of B1-PPF05 beam. On the other hand, once the capacity load was reached for the beams having steel fibers, localized flexural cracks were developed in the maximum moment region with the shear cracks in the tension region (Figure 9). This shear cracks were suddenly propagated along that region as the deflection increased and caused strength loss.

Load-deflection curves of B2 series from experiments and numerical analysis are presented in Figure 10. Crack patterns are given in Figure 11. Similar to B1 control beam, a premature shear failure before yielding of tensile reinforcements was observed in the numerical analysis of B2 control w/o stirrup. The shear strength is almost consistent with the one analytically calculated. Additionally, the failure type can be also confirmed by the shear cracks at the reinforcement layer, which is then extended into the compression zone, Figure 11. Finally, the flexural stiffness before yielding was estimated well.

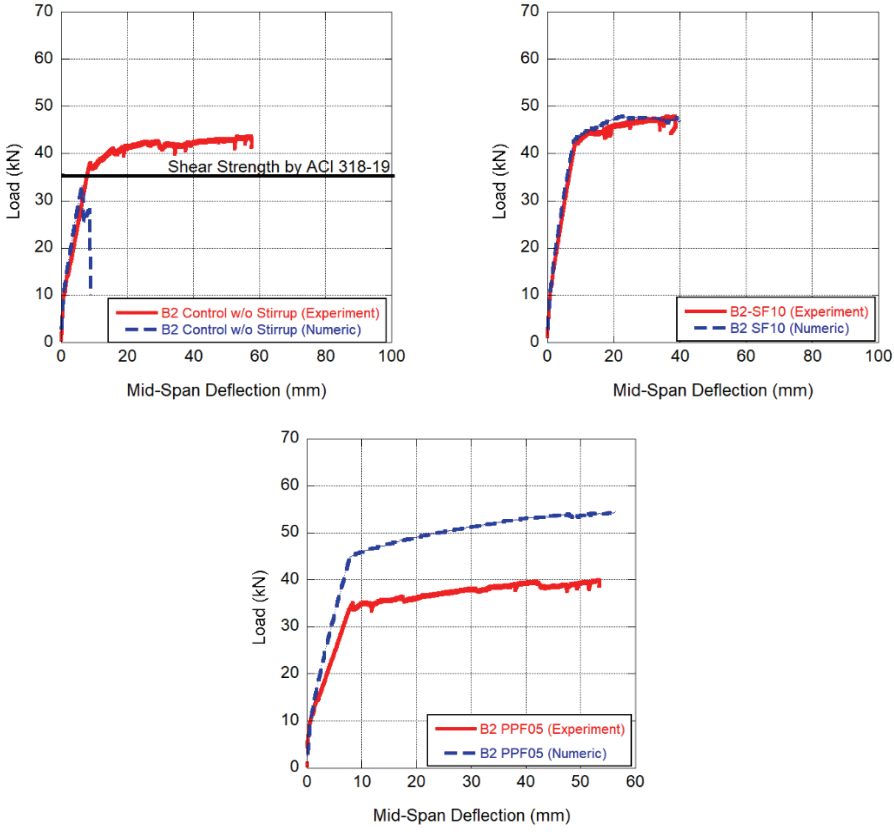

Figure 10 - Comparison of numerical and experimental results for load-deflection curves of B2 series

Identical to B1 series, inclusion of fibers into the beams of B2 series allowed flexural capacity to be fully used for both B2-PPF05 and B2-SF10 beams. The yield strength and the load

carrying capacity of the beam having SF could be estimated precisely. On the other hand, similar to B1-PPF05 beam, they were overestimated for the beam having PPF in the analysis. However, it should be noted that the overestimation exaggerated in B2-PPF05. The flexural stiffness before yielding was investigated next. The numerical analysis results of B2 control and B2-SF10 beams agreed well with that of the experiment while 1.45 times higher stiffness was detected for the beam containing PPF. When it comes to crack patterns, it can be said that once B2-SF10 beam attained the load carrying capacity, a localized flexural crack in the maximum moment region was detected. As the load increased the shear cracks propagated along the tension region.

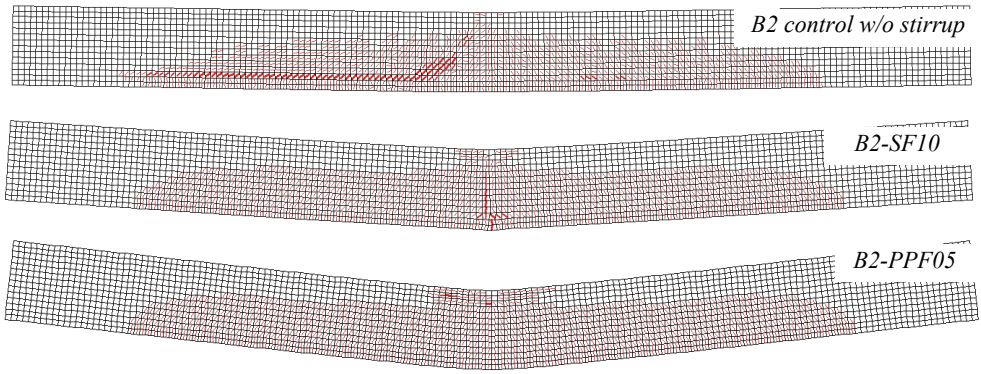

Figure 11 - Crack patterns of B2 series corresponding to peak load

5. CONCLUSION

The effect of fiber type and ratio on the bending behavior of large-scale, doubly reinforced RC beams having various tensile reinforcement ratios that lead to shear and flexural critical designs were investigated experimentally and numerically. Beyond these, the study also aims to provide experimental data into the literature.

The following conclusions can be deduced based on the above discussions.

- In densely reinforced beams (as in B1 series) providing at least 0.5% hooked end steel or PP fiber led the beam specimens to fully use their flexural capacity instead of an enhancement in flexural capacity. However, in lightly reinforced beams (as in B2 series) inclusion of 0.5% PP fibers was not found to be beneficial to improve the flexural capacity. Therefore, the effect of 0.5% fiber content on the behavior was detected to be dependent on the tensile reinforcement ratio.
- Both fiber types with V_f= 0.5% contribute to the shear strength similar to the beam having a minimum amount of stirrup in B1 series. For that reason, replacement of the minimum amount of stirrups according to TS500 by a fiber ratio of at least 0.5% seems feasible in such types of beams as offered in ACI318 code.

- The existence of 1.0% steel fiber was found to be beneficial to improve the flexural strength regardless of the tensile reinforcement ratio. Consequently, the load carrying capacity enhanced by 10% in both beam series.
- Usage of PP fiber was found to be beneficial in improving ductility in the B1 series compared to steel fibers. Moreover, steel fibers substantially decreased the ductility in the B2 series.
- MCFT based nonlinear finite element analysis provided acceptable results in prediction of yield and ultimate strength as well as stiffness before yielding specifically for the beams having steel fiber and stirrup. The behavior could not be estimated accurately for the control beams w/o stirrups. A brittle shear failure was detected, and the tensile reinforcements did not even yield. The reason for this premature failure might be explained by the difference between the actual and assumed tensile strength of concrete material.
- The general trend of load-deflection response of beams having PP fibers in B1 and B2 series could be predicted in good accordance with the experiment. But yield and ultimate strengths were overestimated in the analysis. Therefore, the selected constitutive models for PP fiber reinforced concrete and the second order effects such as tension stiffening were found to be partly successful.

Acknowledgements

This work was supported by the Scientific Research Division of Katip Çelebi University with the grant number 2021-TYL-FEBE-002.

References

[1] Saatçi, S., ve Batarlar, B., Çelik fiber katkılı etriyesiz betonarme kirişlerin davranışı. Journal of the Faculty of Engineering and Architecture of Gazi University, 32:4, 1143-1154, 2017

[2] Folino, P., et. al., Comprehensive analysis of fiber reinforced concrete beams with conventional reinforcement. Engineering Structures, 202, 2020

[3] Amin, A. and Foster, S. J., Shear strength of steel fibre reinforced concrete beams with stirrups. Engineering Structures, 111, 323-332, 2016

[4] Arslan, G., et al. An experimental study on the shear strength of SFRC beams without stirrups. Journal of Theoretical and Applied Mechanics, 55:4, 1205-1217, 2017

[5] Lee, S.,-G., et al. Analysis of steel fiber-reinforced concrete elements subjected to shear. ACI Structural Journal, 113:2, 275-285, 2016

[6] Mahmood, S., M., F., et al. Flexural performance of steel fibre reinforced concrete beams designed for moment redistribution. Engineering Structures, 177, 695-706, 2018

[7] Xu, C., et al. Experimental investigation of the behavior composite steel-concrete composite beams containing different amounts of steel fibres and conventional reinforcement. Construction and Building Materials, 202, 23-36, 2019

[8] Dwarakanath, H., V., and Nagaraj, T., S., Deformational Behavior of Reinforced Fiber Reinforced Concrete Beams in Bending. Journal of Structural Engineering, ASCE, 118:10, 2691-2698, 1992.

[9] Vandewalle, L., Cracking behavior of concrete beams reinforced with a combination of ordinary reinforcement and steel fibers. Materials and Structures, 33, 164-170, 2000.

[10] Dinh, H., H., et al. Shear behavior of steel fiber reinforced concrete beams without stirrup reinforcement. ACI Structural Journal, 107:5, 597-606, 2010

[11] Yoo, D., -Y., et al. Feasibility of replacing minimum shear reinforcement with steel fibers for suitable high-strength concrete beams. Engineering Structures, 147, 207-222, 2017

[12] Abbas, A., A., et al. Shear behavior of steel-fibre-reinforced concrete simply supported beams. Structures and Buildings, 167:SB9, 544-558, 2014

[13] Oh, B., H., Flexural Analysis of Reinforced Concrete Beams Containing Steel Fibers. Journal of Structural Engineering, ASCE, 118:10, 2821-2835, 1992.

[14] Ashour, S., A., et al., Effect of the concrete compressive strength and tensile reinforcement ratio on the flexural behavior of fibrous concrete beams. Engineering Structures, 22, 1145-1158, 2000.

[15] Lim, T-Y., et al., Behavior of Reinforced Steel-Fiber-Concrete Beams in Flexure. Journal of Structural Engineering, ASCE, 113:12, 2439-2458, 1987.

[16] Ning, X., et al., Experimental study and prediction model for flexural behavior of reinforced SCC beam containing steel fibers. Construction and Building Materials, 93, 644-653, 2015.

[17] Wu, Y., Flexural Strength and Behavior of Polypropylene Fiber Reinforced Concrete Beams. Journal of Wuhan University of Technology- Mater. Sci. Ed., 17:2, 54-57, 2002.

[18] Alhozaimy, A., M., et al., Mechanical Properties of Polypropylene Fiber Reinforced Concrete and the Effects of Pozzolanic Materials. Cement and Concrete Composites, 18, 85-92, 1996.

[19] Tutanji, H., A., Properties of polypropylene fiber reinforced silica fume expansive-cement concrete. Construction and Building Materials, 13, 171-177, 1999.

[20] Banthia, N., and Gupta, R., Influence of polypropylene fiber geometry on plastic shrinkage cracking in concrete. Cement and Concrete Research, 36, 1263-1267, 2006.

[21] Sivakumar, A. and Santhanam, M., Mechanical properties of high strength concrete reinforced with metallic and non-metallic fibres. Cement and Concrete Composites, 29, 603-608, 2007.

[22] Hsie, M., et al., Mechanical properties of polypropylene hybrid fiber-reinforced concrete. Materials Science and Engineering A, 494, 153-157, 2008.

[23] Monteiro, V., M., A., M., et al. On the mechanical behavior of polypropylene, steel and hybrid fiber reinforced self-consolidating concrete. Construction and Building Materials, 188, 290-291, 2018

[24] Karimipour, A., and Ghalehnovi, M., Comparison of the effect of the steel and polypropylene fibres on the flexural behavior of recycled aggregate concrete beams. Structures, 29, 129-146, 2021

[25] Vecchio, F. J., and Wong, P., S., VecTor2 & FormWorks User's Manual. 2002

[26] TS500, Requirements for design and construction of reinforced concrete structures. Turkish Standard Institutes, Ankara, 2000

[27] ACI 211.1, Standard practice for selecting proportions for normal, heavyweight and mass concrete, ACI Manual of Concrete Practice, Part 1, 211.1-1 to 211.1-38, 1994

[28] TS802, Design of concrete mixes, Turkish Standard Institute, Ankara, 2016

[29] TS EN 206, Concrete – Specification, performance, production and conformity, Turkish Standard Institute, Ankara, 2014

[30] ACI318, Building code requirements for structural concrete, American Concrete Institute, 2019

[31] TBDY, Türkiye bina deprem yönetmeliği, Afet ve Acil Durum Yönetimi Başkanlığı, Resmî Gazete, 2018

[32] Ersoy, U., Betonarme kiriş ve kolonların moment kapasitelerinin saptanması. İMO Teknik Dergi, 9:44, 1781-1798, 1998

[33] Akan, Ç., Lif katkılı betonarme kirişlerin deneysel ve sayısal incelenmesi. Yüksek Lisans Tezi, İzmir Kâtip Çelebi Üniversitesi, 2022.

[34] Ersoy, U., Özcebe, G. and Tankut, T., Reinforced concrete. METU Press, Ankara, 2016

[35] Sahoo, D., R., et al. Influence of steel and polypropylene fibers on flexural behavior of RC beams. Journal of Materials in Civil Engineering, 27:8, 2015

[36] Meda, A., et al. Flexural behavior of RC beams in fibre reinforced concrete. Composites: Part B, 43:8, 2930-2937, 2012.

[37] Vecchio, F., J., and Collins, M., P., The modified compression-field theory for reinforced concrete elements subjected to shear. ACI Structural Journal, 83:2, 219-231, 1986.